INFLUENCE OF ULTRASONIC TREATMENT ON ELECTROPHYSICAL PROPERTIES OF HgMnTe AND HgCdMnTe SINGLE CRYSTALS

YA.M. OLIKH, S.E. OSTAPOV[1], M.D. TYMOCHKO

UDC 621.315.592.2, 534.2

V.E. Lashkarev Institute of Semiconductor Physics, Nat. Acad. Sci. of Ukraine
(41, Nauky Prosp., Kyiv 03028, Ukraine),

[1]Yu. Fed'kovych Chernivtsi National University
(2, Kotsyubynsky Str., Chernivtsi 58012, Ukraine)

The results of experimental and theoretical studies of how the ultrasonic (US) treatment (UST) and ultrasonic loading (USL) influence HgMnTe and HgCdMnTe semiconductor crystals are reported. It has been demonstrated that the acoustically stimulated changes of electrophysical parameters, namely, (i) an increase of the Hall coefficient $R_{\rm H}$ in specimens with conductivity of the n-type and its reduction in specimens of the p-type and (ii) an increase of the Hall mobility $\mu_{\rm H}$ at high temperatures and its reduction at low ones in specimens of both the n- and p-types are governed (a) by the initial structure of defects in crystals; in particular, an increase of the mercury content results in a reduction of the amplitude threshold of ultrasonic influence; (b) by relations among the contributions made by various mechanisms of current carrier scattering, the most effective US influence being exerted through the mechanism of scattering by ionized impurities; and (c) by the UST parameters such as frequency, intensity, and duration.

1. Introduction

Semiconductors with a small width of the energy gap occupy an important place among the materials which serve as the basis for developing devices that are applied in infrared technical equipment, UHF-electronics, and other areas, with the $Hg_{1-x}Cd_xTe$ (MCT) alloys being mainly used. Nevertheless, the propensity of those materials to lattice, surface, and interface instabilities [1] and, correspondingly, the significant variations of their stoichiometry and charge transfer characteristics, which result from the oxidation of the specimen surface, its mechanical damage, and reactions with metals, are principally problematic for such alloys. Alternative solid solutions $Hg_{1-y}Mn_yTe$ (MMT) at $y \approx 0.1$ and $Hg_{1-x-y}Cd_xMn_yTe$ (MCMT) at $x \approx 0.14$ and $y \approx 0.03$ possess the same width of the energy gap as MCT at $x = 0.2$ and the mobility of electrons that exceeds 10^6 cm^2/(V $\cdot$ s) at low temperatures [2]. In this case, the presence of manganese ions stabilizes unstable chemical bonds in the HgTe crystal lattice and provides a higher structural perfection of MMT crystals, which makes them advantageous, to a certain extent, in the manufacture of multicomponent optical systems [3].

In the course of crystal growing, various macroscopical inhomogeneities of growth arise. These inhomogeneities generate interconnected mechanical and electric fields, which ultimately stimulates long-term relaxation processes in the crystal. These processes, in turn, are the origin of a spread of specimen's parameters and, in particular, of their functional individuality at intense influences. Therefore, there is a necessity for the control over irreversible variations of these internal fields in a crystal, both at the stage of technological treatment of specimens and during the operation of detectors created on their basis [4]. The application of ultrasound in the course of researches expands methodical opportunities for the diagnostics of semiconducting materials and semiconductor-based devices. In particular, as was found for $Hg_{1-x}Cd_xTe$, the UST makes it possible to modify their defective structure by varying the electrically and optically active defects in a crystal [5, 6]. For example, it is possible to reduce mechanical stresses in specimens, which arise in the course of material growing and processing, to decrease the concentration of intrinsic point defects, to intensify the process of diffusion of doping impurities, and to improve the stability of crystal parameters [6, 7]. As the mechanism of US influence has the acoustical and dislocation-related origin, and the structures of dislocations and small-angle interfaces in MCT, MMT and MCMT crystals are similar, we may expect that such acoustically stimulated effects may manifest themselves in those crystals.

This work aimed at obtaining the information about electrophysical characteristics of MMT and MCMT specimens with various degrees of structural perfection and elucidating the mechanisms of acoustically stimulated formation of defects in them in connection

with the parameters of the US modes, i.e. a long UST and a USL.

2. Specimens and Experiment

For researches, we used MCMT single crystals of the n-type and MMT ones of the p-type of conductivity, grown by the modified method of zone melting in the rotating ampoules inclined to the horizon [8, 9]. The contents of cadmium and manganese at the synthesis were such that the width of the energy gap at the temperature of liquid nitrogen was $E_g \approx 0.1$ eV. It ensured the prospects of the material for the optical detecting of radiation in the range $\lambda = 8 \div 14$ μm.

Specimens for researches were cut off in the form of rectangular $(6 \div 11) \times (1 \div 2) \times (0.6 \div 1.5)$-mm^3 parallelepipeds from wafers up to 2 mm in thickness and subjected to a chemical and mechanical treatment usual for MCT, which removed the near-surface layers damaged during the cutting of wafers. The characteristics of specimens are quoted in the Table.

In the course of researches, we measured the temperature dependences of the Hall coefficient $R_{\rm H}(T)$ and the electroconductivity $\sigma(T)$ at a constant magnetic field $B = 0.45$ T within a temperature interval of $80-300$ K, and calculated the temperature dependences of the Hall mobility of current carriers $\mu_{\rm H}(T) = R_{\rm H}(T)\sigma(T)$. The specimens were treated during $t_{\rm US} = 10^3 \div 10^4$ s by longitudinal US waves with the frequencies $f_{\rm US} = 5 \div 17$ MHz, the intensities $W_{\rm US} = 0.1 \div 1$ W/cm^2, and propagating along the $\langle 111 \rangle$ direction in the crystal. Measurements were carried out after every treatment stage. In the process of *in situ* measurements of $R_{\rm H}(T)$ and $\sigma(T)$, dynamical USL ($W \sim 0.1$ W/cm^2) was also used.

3. Calculation of the Temperature Dependence of Current Carrier Mobility

While simulating the temperature dependence of the current carrier mobility in narrow-gap semiconducting materials, such as MCT, we considered three basic mechanisms of current carrier scattering: by ionized impurities, acoustic phonons, and optical phonons [8–10]. Scattering by ionized impurities was taken into account making use of the Brooks–Herring formula [11]

$$\mu_I = \frac{2^{7/2}\kappa^2(4\pi\varepsilon_0)^2(k_0T)^{3/2}}{\pi^{3/2}N_I e^3 (m^*)^{1/2}\ln y}, \qquad (1)$$

where

$$\ln y = \ln(1+b) - b/(1+b), \quad b = \frac{6\kappa(4\pi\varepsilon_0)m^*(k_0T)^2}{\pi p^*\hbar^2 e^2},$$

$$p^* = p + (p+N_D)[1-(p+N_D)/N_A],$$

$N_I = p + 2N_D$, κ is the dielectric permittivity, and ε_0 the dielectric constant of the crystal.

The mobility of current carriers under their scattering by crystal lattice vibrations was estimated with the use of the corresponding time of relaxation [8,9]: by optical phonons

$$\tau_{\rm opt} = \frac{\varepsilon_0 h}{2e^2 k_0 T}\,\frac{\partial E}{\partial k}\,\frac{1}{F_{\rm opt}}, \qquad (2)$$

Parameters of $Hg_{1-y}Mn_yTe$ and $Hg_{1-x-y}Cd_xMn_yTe$ specimens

Specimen $[E_g(77\ {\rm K})/E_g\ (300\ {\rm K})]$, eV	x y	Curve number in the figures	Specimen treatment mode	N_a, 10^{15} cm^{-3}	N_d, 10^{15} cm^{-3}	$(N_a - N_d)$ 10^{15} cm^{-3}
p-8.1M	0	1	initial	100	20	80
[0.05/0.17]	0.083	2	UST-1	350	27	323
		3	UST-2	750	45	705
p-8.2M	0	1	initial	70	30	40
[0.05/0.17]	0.08	2	UST-1	90	60	30
		1	initial	5	4.5	0.5
n-4.4	0.12	2	UST-1	5.3	4.9	0.4
[0.022/0.1]	0.02	3	UST-2	20	19	1.0
		4	UST-3	30	29	1.0
n-4.39O	0.12	1	initial	55	30	25
[0.022/0.1]	0.03	3	UST-2	130	52	78
n-4.39H	0.12	1	Without US	95	30	65
[0.022/0.1]	0.03	2	US-1(*in situ*)	65	30	35

*Notations: UST-1 means $f_{\rm US} = 13$ MHz, $W_{\rm US} = 0.1$ W/cm^{-2}, and $t_{\rm US} = 2\times10^3$ s; UST-2 means $f_{\rm US} = 13$ MHz, $W_{\rm US} = 0.5$ W/cm^{-2}, and $t_{\rm US} = 7\times10^3$ s; UST-3 means $f_{\rm US} = 13$ MHz, $W_{\rm US} = 1$ W/cm^{-2}, and $t_{\rm US} = 7\times10^3$ s; N_a and N_d are the calculated values of the acceptor and donor concentrations, respectively

and by acoustic phonons

$$\tau_{\rm ac} = \frac{\pi h \rho(y) v^2}{E_0^2 k_0 T F_{\rm ac}} \frac{\partial E}{\partial k} \frac{1}{k^2}. \qquad (3)$$

Here, $\rho(y)$ is the crystal density which depends on the contents of cadmium and manganese; for example, $\rho(y) = 8.12 - 3.37y$ for MMT; E_0 is the constant of the deformation potential; and $F_{\rm ac}$ and $F_{\rm opt}$ are the functions which make allowance for the influence of Bloch factors in the Kane model of scattering for acoustic and polar optical phonons, respectively [12]. For example, for $Mn_{0.08}Hg_{0.92}Te$ at $T = 300$ K, $\rho(0.08) = 7.85$ g/cm^{-3}, $E_0 \approx 10$ eV, $F_{\rm ac} \approx 0.4$, and $F_{\rm opt} \approx 0.6$.

The energy gap width E_g and the concentration of intrinsic current carriers n_i were calculated by the corresponding empirical formula presented for MMT in work [13] and for MCMT in work [14].

The results of calculations of the current carrier mobility, made according to the method indicated above, and their comparison with experimental data for MCMT specimen n-4.4 are shown in Fig. 1,*a*. It is evident that the account of three considered mechanisms of scattering was sufficient for a rather exact simulation of the current carrier mobility. The scattering by ionized impurities prevailed at low temperatures (70 – 100 K), while, as the temperature grew up to room one, the contribution of crystal lattice vibrations increased. We see that, in this case, acoustic phonons made no essential contribution to the current carrier scattering within the whole temperature range. The results of the mobility simulation for temperatures, at which the scattering by ionized impurity dominated, were used to evaluate the impurity concentration. For several specimens, we failed to reach the domination of the impurity scattering and to determine its contribution in an explicit form by the method described above. In such cases, we simulated the mobility and the specific conductivity in the whole temperature range (Fig. 1,*b*). The values of N_a and N_d were estimated provided the best fitting of experimental data by theoretical curves. The results of such evaluations are displayed in the Table.

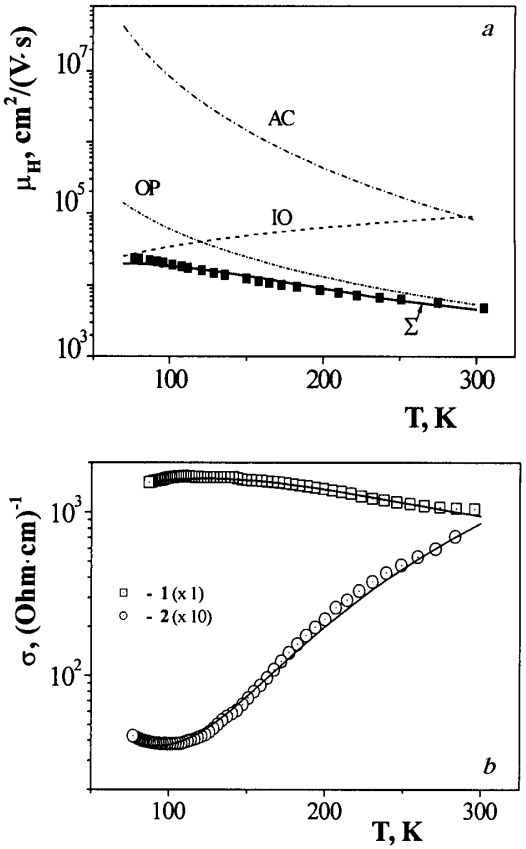

Fig. 1. *a* — temperature dependences of the Hall mobility of current carriers scattered by acoustic phonons (*AC*), ionized impurities (*IO*), optical phonons (*OP*), and taking into account all three mechanisms of scattering (Σ); points are the experimental data for the specimen n-CdMnHgTe-4.4. *b* — temperature dependences of the specific conductivity for the p-MnHgTe 8.2M (*1*) and n-CdMnHgTe 4.39H (*2*) specimens

4. Experimental Results and Their Discussion

The results of experimental researches of the specimens after their UST and in the course of USL are presented in Figs. 2–6. In Figs. 2 and 3, the temperature dependences of the Hall coefficient, the specific conductivity, and the current carrier mobility before and after several cycles of UST of MMT specimens of the p-type cut off from the same ingot are shown. The initial specimen p-8.2M, after its preliminary γ-irradiation by Co^{60} (the irradiation dose was $D \leq 10^9$ rad), was characterized by somewhat lower values of N_a (see the table) and higher values of the Hall mobility and the specific conductivity than the specimen p-8.1M. One can see that slightly different initial conditions resulted in a qualitative difference between the UST results. While the specimen p-8.1M demonstrated a reduction of both the current carrier mobility and the Hall coefficient, as well as an increase of the specific conductivity, the specimen p-8.2M revealed almost no change of the current carrier mobility after the treatment. It can be due to a γ-radiation-induced reduction of the initial concentration of electrically active, i.e. ionized, defects (EADs). In this case, the contribution of the scattering by ionized impurities was

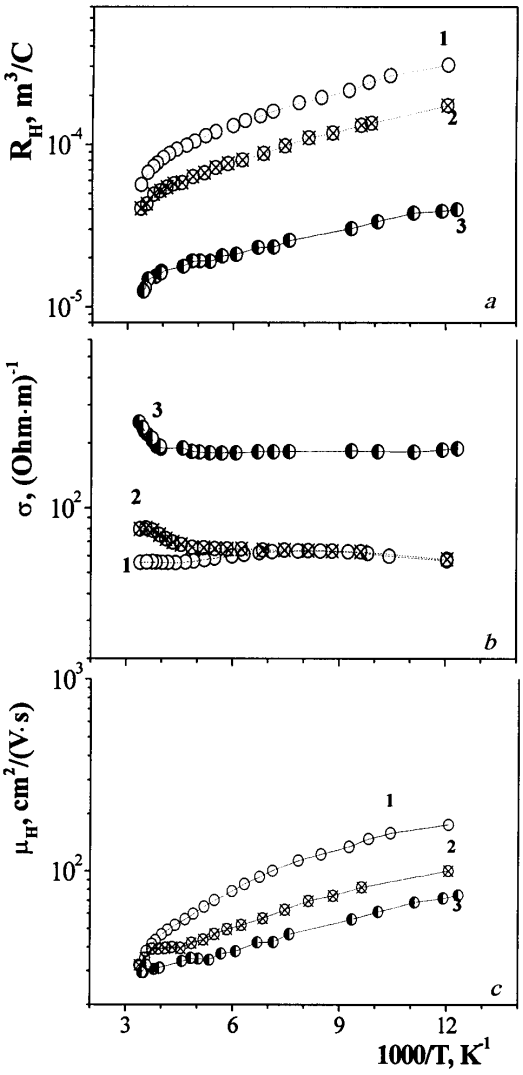

Fig. 2. Temperature dependences of the Hall coefficient R_{H} (a), the specific conductivity σ (b), and the Hall mobility μ_{H} (c) for the initial and US-treated p-MnHgTe 8.1M specimen. The numbering of the curves is quoted in the Table

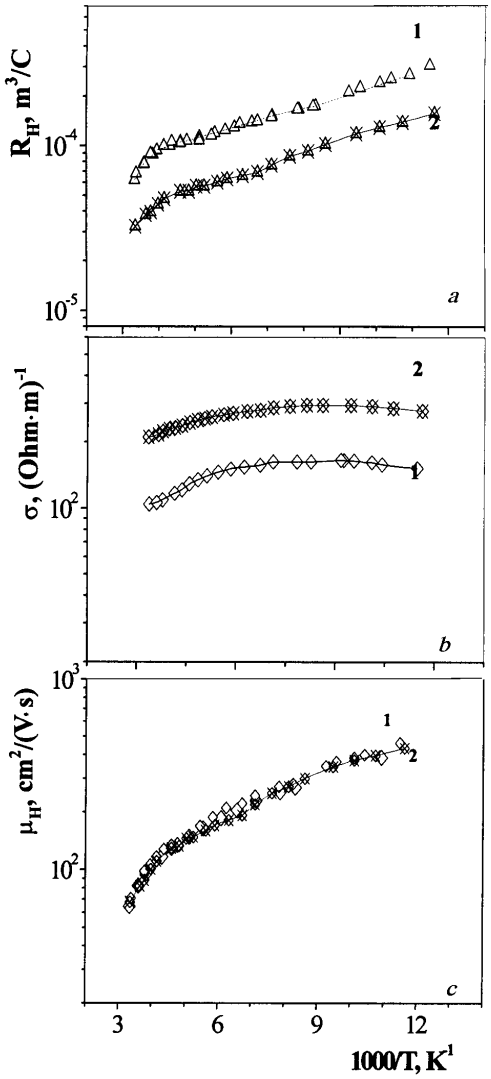

Fig. 3. The same as in Fig. 2 but for the p-MnHgTe 8.2M specimen

rather small (see Fig. 3,c) and did not manifest itself even after UST. In order to estimate the EAD concentration for this specimen, we simulated its specific conductivity (see Fig. 1,b). One can see that the simulation resulted in a satisfactory agreement between theoretical calculations and experimental data, which allowed us to determine N_a and N_d. Therefore, the influence of UST resulted in an increase of N_a and N_d, with $\sigma(T)$ for the specimen p-8.2M remaining lower than that for the specimen p-8.1M even after the former having been subjected to UST. All this evidences for the same character of the UST influence on both specimens of the p-type.

Figs. 4 and 5 present the results of UST of two MCMT specimens which were also cut off from the same ingot. Despite this circumstance, they revealed rather different electrophysical characteristics. For example, the specimen n-4.4 had conductivity of the n-type, the temperature dependences of the Hall coefficient and the specific conductivity typical of narrow-band-gap semiconductors, and a rather high mobility of current carriers ($\mu_{\mathrm{H}} \approx 10^4$ cm^2/(V · s) at $T = 80$ K) in the whole temperature range. At the same time, the specimen n-4.39O was characterized by inversion of the Hall coefficient, i.e. it had conductivity of the p-type at low

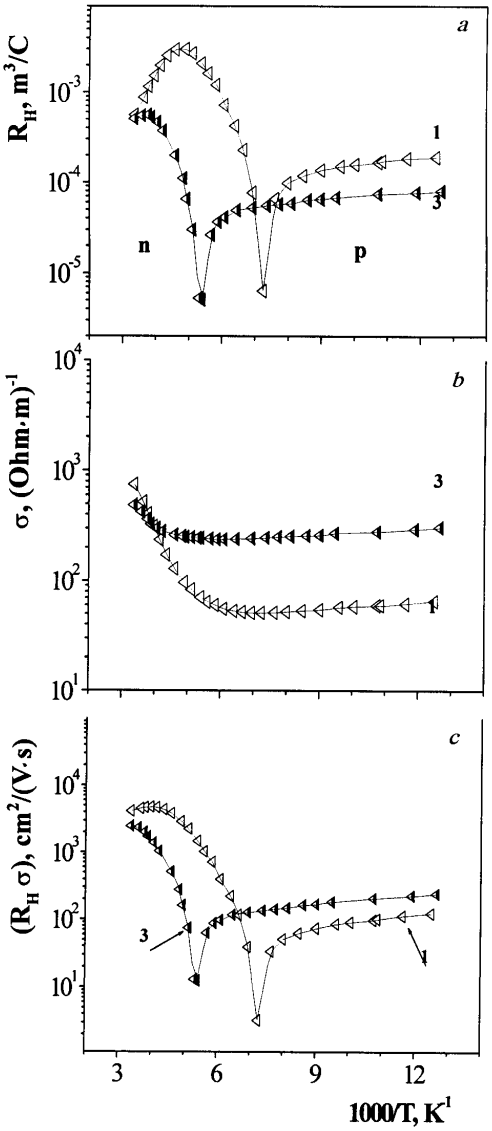

Fig. 4. The same as in Fig. 2 but for the n-CdMnHgTe 4.39O specimen

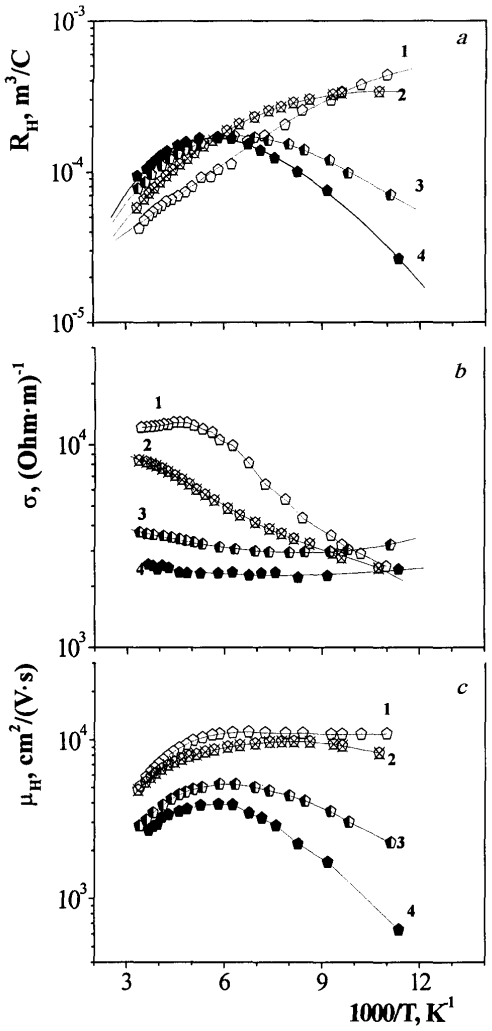

Fig. 5. The same as in Fig. 2 but for the n-CdMnHgTe 4.4 specimen

temperatures and that of the n-type at high ones. The mobility of current carriers in this specimen was lower than that in the specimen n-4.4. All this together testified to that the EAD concentration in the n-4.39O was much higher than that in the specimen n-4.4 (see the Table). We note that both the specimens were compensated. UST of the specimen n-4.39O resulted in a shift of the temperature of inversion of $R_{\rm H}$ by about 60 K towards higher temperatures (Fig. 4, curve *3*). A similar acoustically induced shift of the maximum of the dependence $R_{\rm H}(T)$ and an increase of its slope after further UST cycles were also observed for the specimen n-4.4 (Fig. 5, curves *2–4*). A certain approach of the dependence $R_{\rm H}(T)$ for the specimen n-4.4 to the relevant dependence for the specimen n-4.39O (Fig. 4, curve *1*) occurred in this case. In the course of UST, the conductivity gradually decreased, because the number of defects of acceptor type (vacancies and dislocations) and, accordingly, the degree of compensation increased. The growth of the electron scattering by newly created ionized defects was evidenced for by a reduction of the electron mobility. Therefore, an increase of the intensity and a prolongation of UST of the specimens n-4.4 and n-4.39O were accompanied by a rapid generation of additional vacancy defects (see the Table). In so doing, UST of the specimen n-4.4 approached its $R_{\rm H}(T)$

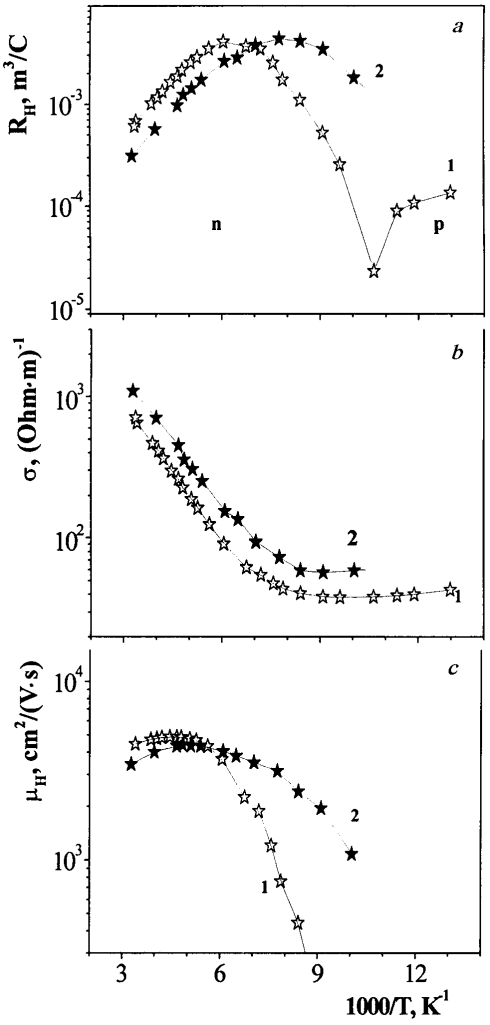

Fig. 6. Temperature dependences of the Hall coefficient $R_{\rm H}$ (a), the specific conductivity σ (b), and the Hall mobility $\mu_{\rm H}$ (c) for the initial and US-loaded n-CdMnHgTe 4.39H specimen. The numbering of the curves is quoted in the Table

dependence to the corresponding dependence of the initial specimen n-4.39O. Further USTs of specimen n-4.4 can lead to the inversion of its dependence $R_{\rm H}(T)$ in the researched temperature interval. The generation of additional (UST-induced) defects in those specimens resulted in a decrease of $\mu_{\rm H}$ in the low-temperature region.

Thus, UST of specimens with a mixed or n-type of conductivity results in an increase of the difference $N_a - N_d$, which makes a specimen with conductivity of the n-type "less electronic" and shifts the point of inversion of the Hall coefficient towards higher temperatures. Moreover, a decrease of the slope of the curve $\mu_{\rm H}(T) = AT^r$ in the high-temperature region may evidence for some changes in the character of the phonon scattering, namely, an enhancement of its acoustic component.

The results of the dynamical influence of USL on the electrophysical characteristics of a MCMT crystal are shown in Fig. 6; the measurements being carried out *in situ* during the loading procedure. We note that dynamical variations of the dependences $R_{\rm H}(T)$ and $\sigma(T)$ in the course of USL are reversible as opposed to the UST effects, when the acoustically stimulated changes of the electrophysical parameters of specimens were irreversible. From Fig. 6, one can see that the maxima of the dependences $R_{\rm H}(T)$ and $\sigma(T)$ are shifted towards low temperatures, so that the inversion temperature is also shifted in this direction. Such a character of the behavior of $R_{\rm H}(T)$ and $\sigma(T)$ in the course of USL is different from and even opposite to that obtained in the course of a stationary UST.

The difference between the results of the stationary and dynamical US actions is explained, in our opinion, by different values of the diffusion coefficient of mercury atoms $D_{\rm Hg}$ under these conditions [15]. As UST was carried out at room temperature, the value of $D_{\rm Hg}$ was rather high, so that newly created interstitial Hg atoms had enough time to diffuse to dislocations and to be fastened there. At the same time, new Hg vacancies, being the other component of the Frenkel pair and owing to their much lower value of $D_{V_{\rm Hg}}$, remained in the crystal bulk, thus increasing the concentration N_a. Such an influence of UST has been investigated earlier on $Hg_{1-x}Cd_xTe$ crystals [5, 6, 10].

On the other hand, the measurements in the course of USL were carried out at much lower temperatures and during short terms. Therefore, the value of $D_{\rm Hg}$ was low, the acoustically stimulated generation of pairs (interstitial Hg atom – Hg vacancy) occurred only during the US action, so that the components were situated at a short distance. After the ultrasound having been switched off, the components recombined during a short period, and the characteristics of the specimen came back to the initial state. This means that the action of USL was reversible. It is clear that the character of a variation of $\mu_{\rm H}(T)$ was also defined by the real (dynamical and statistical) concentration and the structure of defects in the crystal lattice of a specimen.

After a long-term UST, additional point defects are inserted, which results in a decrease of $\mu_{\rm H}$ and a certain redistribution among the contributions of various mechanisms to the scattering. Therefore, the essence of the UST processes comprises a redistribution of initial (intrinsic) and newly generated point defects between the matrix and drains (dislocations, small-angle

interfaces, subblock interfaces, and so on), the latter being determined by the initial state of the defect system and resulting in modifications of the material properties. In accordance with the general regularities of the defect formation in both MCT [11, 14–16] and MMT, if the concentration of point defects on dislocations is high, which is typical of specimens annealed in an atmosphere of mercury, the UST may be accompanied by the tearing of excess (as compared to the volume) defects, e.g., Hg_i atoms, away from dislocations into interstitial spaces of the crystalline matrix and/or by the capture of vacancies by linear defects [10, 15]. In this case, N_d may increase and N_a may decrease. In another case, where drains are not saturated by Hg_i atoms, the influence of UST comes to the intense generation of electrically active centers (see above). The process of this kind is characterized by a growth of N_a in specimens of the p-type (see the Table).

Conclusions

1. The acoustically stimulated changes of electrophysical properties, namely, an increase of the Hall coefficient R_H in specimens with conductivity of the n-type and its reduction in specimens of the p-type, and an increase of the Hall mobility of current carriers μ_H in the high-temperature region and its reduction in the low-temperature one in specimens with conductivity of both the n- and p-types, are ambiguous and governed by several factors:

- by the initial structure of both intrinsic point-like and linear defects in the crystals under investigation; for example, an increase of the mercury content reduces the amplitude threshold of the US influence;
- by change of the relative contributions of various mechanisms of current carrier scattering; for examlpe, both the scattering by ionized impurities and the contribution of the scattering by acoustic phonons increase;
- by the parameters (frequency, intensity, and duration) of the US treatment.

2. The mechanism of the US influence has a dislocation nature. The basic changes of electrophysical parameters are connected with a redistribution of Hg atoms between the crystal bulk and dislocations in the course of acoustically stimulated vibrations of the latter.

3. The US treatment and the US loading allow one to use ultrasound for simulating and monitoring the transport properties of specific specimens of $Hg_{1-y}Mn_yTe$ and $Hg_{1-x-y}Cd_xMn_yTe$.

The authors thank O.O. Bodnaruk (Chernivtsi National University) for the crystals presented for our researches.

1. *Spicer W.E., Silberman J.A., Lindau J. et al.* // J. Vac. Sci. and Technol. A. — 1983. — **1**, N 3. — P. 1735 — 1743.
2. *Furdina J.K.* // Proc. Intern. Soc. Opt. Eng. — 1983. — **409**, N 43. — P. 43 — 52.
3. *Wall A., Caprile C., Fraciosi A.* // J. Vac. Sci. and Technol. A. — 1986. — **4**, N 3. — P. 818 — 822.
4. *Klimenko I.A., Migal' V.P., Komar' V.K. et al.* // Proc. Intern. Conf. on Sensor Electronics and Microsystem Technologies, June 1—5, 2004, Odesa,. Ukraine. — P. 281.
5. *Baranskii P.I., Belyaev A.E., Komirenko S.M., Shevchenko N.V.* // Fiz. Tverd. Tela. — 1990. — **32**, N 7. — P. 2159 — 2161.
6. *Vlasenko A.I., Olikh Ya.M., Savkina R.K.* // Fiz. Tekhn. Polupr. — 1999. — **33**, N 4. — P. 410 — 414.
7. *Garyagdyev G., Gorodetskii I.Ya., Dzhumaev B.R. et al.* // Ibid. — 1991. — **25**, N 3. — P. 409 — 412.
8. *Kosyachenko L.A., Markov A.V., Ostapov S.E. et al.* // Zh. Fiz. Dosl. — 2003. — **7**, N 1. — P. 101 — 105.
9. *Bodnaruk O.O., Ostapov S.E., Rarenko I.M., Tymochko M.D.* // J. Alloys and Compounds. — 2004. — **371**, N 1—2. — P. 93 — 96.
10. *Vlasenko A.I., Olikh Ya.M., Savkina R.K.* // Fiz. Tekhn. Polupr. — 2000. — **34**, N 6. — P. 670 — 675.
11. *Scott W., Stelzer E., Hager J.* // J. Appl. Phys. — 1976. — **47**, N 4. — P. 1408 — 1414.
12. *Beketov G.V., Belyaev A.E., Vitusevich S.A. et al.* // Fiz. Tekhn. Polupr. — 1997. — **31**, N 3. — P. 268 — 272.
13. *Rogalski A.* // Infrared Phys. — 1991. — **31**. — P. 117 — 166.
14. *Bodnaruk O.A., Markov A.V., Ostapov S.E. et al.* // Fiz. Tekhn. Polupr. — 2000. — **34**, N 4. — P. 430 — 432.
15. *Olikh Ya.M., Shavlyuk Yu.I.* // Fiz. Tverd. Tela. — 1996. — **38**, N 2. — P. 468 — 473.
16. *Franciosi A., Philip P., Peterman D.J.* // Phys. Rev. B. — 1985. — **32**, N 12. — P. 8100 — 8107.

Received 06.12.04.
Translated from Ukrainian by O.I.Voitenko

ВПЛИВ УЛЬТРАЗВУКОВОЇ ОБРОБКИ НА ЕЛЕКТРОФІЗИЧНІ ВЛАСТИВОСТІ МОНОКРИСТАЛІВ HgMnTe ТА HgCdMnTe

Я.М. Оліх, С.Е. Остапов, М.Д. Тимочко

Р е з ю м е

Проведено експериментальні та теоретичні дослідження впливу ультразвукової обробки (УЗО) та УЗ-навантаження (УЗН)

на напівпровідникові кристали HgMnTe та HgCdMnTe. Показано, що акустостимульовані зміни електрофізичних параметрів, а саме: збільшення коефіцієнта Холла $R_{\rm H}$ у зразках n-типу провідності і зменшення його у зразках p-типу, збільшення холлівської рухливості $\mu_{\rm H}$ у високотемпературній і зменшення у низькотемпературній областях для зразків як для n-, так і для p-типу провідності, — визначаються а) вихідною структурою дефектів кристалів (зі збільшенням вмісту Hg знижується амплітудний поріг УЗ-впливу), б) відносним внеском різних механізмів розсіювання носіїв заряду (найбільш ефективний УЗ-вплив здійснюється за механізмом розсіювання на іонізованих домішках), в) режимами УЗ (частотою, інтенсивністю та тривалістю).